Vineyard irrigation scheduling based on airborne thermal imagery and water potential thresholds

J. BELLVERT[1], P.J. ZARCO-TEJADA[2], J. MARSAL[1], J. GIRONA[1], V. GONZÁLEZ-DUGO[2] and E. FERERES[2,3]

[1] Efficient Use of Water Program, Institut de Recerca i Tecnologia Agroalimentàries (IRTA), 25003 Lleida, Spain; [2] Instituto de Agricultura Sostenible (IAS), Consejo Superior de Investigaciones Científicas (CSIC), 14004 Córdoba, Spain; [3] Department of Agronomy, University of Córdoba (UCO), 14014 Córdoba, Spain
Corresponding author: Dr Joaquim Bellvert, email joaquim.bellvert@irta.cat

Abstract

Background and Aims: Mapping the spatial variability of vine water status within a vineyard is necessary for the efficient management of irrigation water. The objective of this study was to determine whether estimates of remotely sensed leaf water potential (Ψ_{rem}) could be employed as a precise tool for scheduling irrigation at the irrigation sector level throughout the season.
Methods and Results: Three irrigation treatments were applied in a 16-ha commercial vineyard to analyse the performance of the proposed methodology for monitoring regulated deficit irrigation strategies, and to evaluate the required frequency of the acquisition of thermal images for irrigation scheduling. An aircraft equipped with a thermal sensor flew over the vineyard throughout the season, and the averaged Ψ_{rem} of each irrigation sector was used as the irrigation trigger. The acquisition of about five or six Ψ_{rem} maps over the season is recommended. The starting date for acquiring thermal images depends on canopy vegetation size and on the difficulty of extracting pure vegetation pixels. The effect of acquiring thermal imagery on days after rainfall or with low vapour pressure deficits affected the estimation of Ψ_{rem}, and these constraints need to be considered for feasible irrigation purposes.
Conclusions: Remotely sensed leaf water potential was successfully used as an irrigation trigger to adopt regulated deficit irrigation strategies without any negative effect on yield and wine composition.
Significance of the Study: This study presented a promising and powerful method for scheduling irrigation throughout the season at vineyard level based on estimates of remotely sensed leaf water potential.

Keywords: *crop water stress index, leaf water potential, remote sensing, thermal imagery, winegrapes*

Introduction

The composition of winegrapes for producing wine is dependent on the history of vine water status during the growing season (Ginestar et al. 1998, Girona et al. 2006, Intrigliolo and Castel 2010). Controlling vine water status throughout the season is a requisite for adopting the most appropriate irrigation strategy for each cultivar (Girona et al. 2009, van Leeuwen et al. 2009, Basile et al. 2011). Leaf water potential (Ψ_L) is regarded as the most standard indicator for plant water status and has been proposed for scheduling irrigation in commercial vineyards (Girona et al. 2006). Characterisation of the water status, however, over the whole vineyard needs individual leaf measurements, and is therefore time-consuming and costly. This limits the suitability of this system for application over large areas.

Mapping the spatial variability of vine water status is especially important for improving efficient irrigation within a vineyard, but constitutes a major challenge. Significant variability of the vine water status within vineyards has already been shown under irrigated and non-irrigated conditions (Ojeda et al. 2005, Acevedo-Opazo et al. 2010, Bellvert et al. 2012). The variability that is generally observed in the field implies differences in plant growth and in water requirements in different zones within the vineyard. If irrigation is scheduled only by using the water balance method (Allen et al. 1998) and without taking into account vineyard heterogeneity, this may result in water being wasted in some parts of the vineyard, while there may be an insufficient water supply in other parts. Vineyard spatial heterogeneity will affect vegetative growth, yield and berry composition (Bramley and Hamilton 2004, Bramley et al. 2005, Bellvert et al. 2012). Plant water status indicators, if used judiciously, may possibly reduce heterogeneity and irrigation inefficiencies.

The use of thermal information for detecting plant water status became popular in the 1960s with the use of thermal-infrared sensors at ground level (Tanner 1963, Fuchs and Tanner 1966). In the 1980s, Idso and co-workers developed the concept of the crop water stress index (CWSI) (Idso et al. 1981, Jackson et al. 1981), which is the most commonly used plant water status indicator derived from canopy temperature. This index is based on relating canopy-air temperature difference (T_c–T_a) to air vapour pressure deficit (VPD) (Idso et al. 1981). The extensive use of CWSI, however, for water stress detection of large areas did not occur until more recently with the introduction of state-of-the-art technology and the integration of high-resolution thermal cameras on board manned (Sepulcre-Cantó et al. 2006, 2007) and unmanned aerial vehicles (Berni et al. 2009a,b, Zarco-Tejada et al. 2009, Bellvert et al. 2014a). Remotely sensed CWSI has been successfully related with Ψ_L for different winegrape cultivars (Grimes and Williams 1990, Möller et al. 2007, Bellvert et al. 2014b). The large-scale use of CWSI, however, as an indicator to trigger irrigation has not been widely adopted throughout a complete season for several reasons: (i) the correlation between CWSI and Ψ_L may differ between phenological stages and cultivars (Bellvert et al. 2014b), so research is needed to assess accurately these relationships; (ii) most airborne sensors lack the necessary spatial resolution for the accurate separation of canopy temperature

doi: 10.1111/ajgw.12173

and shaded soil background (Berni et al. 2009a, Bellvert et al. 2014a); (iii) the need to obtain images on a weekly basis (the low turnaround time and repeat cycle of satellite-based platforms have limited their usefulness for crop management; Berni et al. 2009b); and (iv) the empirical approach to calculating CWSI has a degree of site specificity. In general, it appears that an unreliable CWSI may be obtained when the VPD is lower than 2 kPa (Hipps et al. 1985, Testi et al. 2008).

The objective of this study was to determine whether remotely sensed leaf water potential (Ψ_{rem}) estimated from CWSI could be employed as a precise tool for taking irrigation decisions in vineyards at the irrigation sector level by using them to detect vine water status throughout the season. To our knowledge, no studies have been published on the possibility of scheduling irrigation of a vineyard throughout the season based on the use of Ψ_{rem}. This study was based on detecting a difference between full irrigation (100% crop evapotranspiration, ETc) and regulated deficit irrigation (RDI) strategies, which were adopted by combining information from the water balance method with adjustments based on Ψ_L thresholds. In addition, the necessary frequency to acquire airborne thermal imagery for irrigation scheduling proposals was also determined.

Materials and methods

Study site

The study was carried out in 2012 in a 16-ha commercial Chardonnay vineyard located at Raimat, Lleida, Spain (41°39′43″N, 0°30′16″E). Vines were planted at a spacing of 2.0 m × 3.0 m (1667 vines/ha). They were cordon-trained to a vertical shoot position canopy system at a height of 0.9 m. Canopy dimensions were maintained by vertical shoot positioning in July and hedging shoots above the top wire twice during the growing season. The soil of the site is of silty-loam texture (US Department of Agriculture-Soil Conservation Service 1975). The climate in the area is semi-arid, characterised by warm, dry summers, and cool, wet winters, with an annual rainfall and ET_o, respectively, of 355 mm and 1094 mm, for 2012. The irrigation system was divided into 12 regular sectors of between 1.0 and 1.6 ha each (Figure 1). Pressure compensating drip emitters with a nominal flow of 2.3 L/h were spaced 0.85 m apart. The system was operated by an irrigation controller that individually opened and closed the solenoid valves corresponding to each irrigation sector. Vines were automatically irrigated daily and scheduled on a weekly basis.

Irrigation treatments

Three irrigation treatments were applied in this experiment. Irrigation was scheduled to satisfy full water requirements in three sectors (control), while a deficit irrigation (RDI) strategy was imposed in the remaining sectors. Regulated deficit irrigation was scheduled by using leaf water potential thresholds (Ψ_{thr}) throughout the growing season and consisted of reducing water allocation during stage II (full fruitset to 50% veraison). Leaf water potential threshold was defined for the RDI treatments according to the optimal values provided by Basile et al. (2012) for obtaining high-quality Chardonnay wines. The irrigation schedule conducted in the experiment comprised the following three treatments: (i) control, where irrigation was scheduled to satisfy full requirements by using the water balance method; (ii) RDI-W, with an RDI strategy during stage II, and irrigation scheduled on a weekly basis; and (iii) RDI-BW, similar to RDI-W, but with irrigation scheduled once every 2 weeks. The established Ψ_{thr} for the RDI treatments was −0.8 MPa from anthesis to full fruitset (stage I); −1.1 MPa from full fruitset to 50% veraison (stage II); and −0.9 MPa from the end of stage II to harvest (stage III). During the postharvest period, irrigation scheduling consisted of satisfying full irrigation requirements for all treatments. The RDI-W and RDI-BW treatments were each applied in four irrigation sectors. Besides these treatments, a final irrigation sector was included for comparison purposes, which considered more severe irrigation conditions. In this sector, severe water deficit was applied from the beginning of stage II until harvest on a weekly basis (DI-W). The purpose was to reach a Ψ_{thr} of −1.2 MPa.

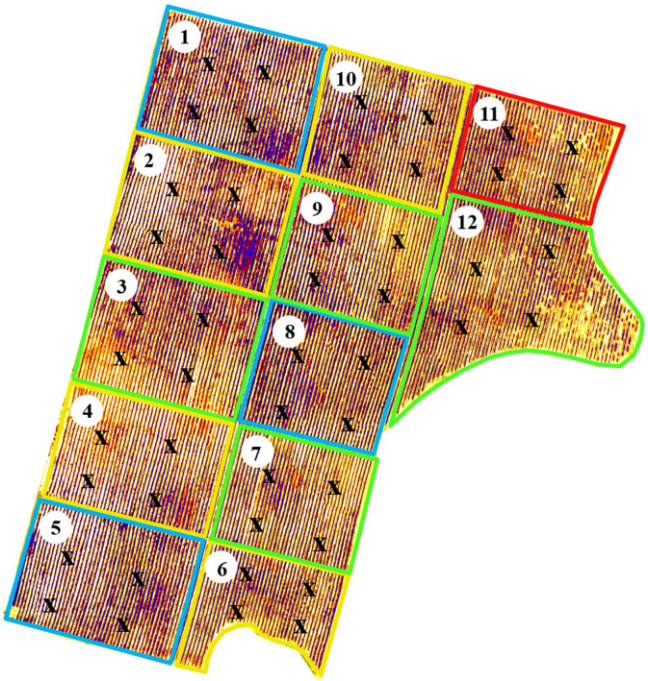

Figure 1. Thermal image overview of a 16-ha commercial Chardonnay vineyard showing the irrigation sectors, with a random distribution of the three irrigation treatments: control (□); RDI-W, regulated deficit irrigation with a weekly scheduling (□); and RDI-BW, regulated deficit irrigation with a biweekly scheduling (□) and of one sector subjected to severe deficit irrigation on a weekly basis (DI-W) (□). **X** indicates the location of vines whose leaf water potential (Ψ_L) was measured.

Each irrigation treatment was conducted at irrigation-sector scale, and the experimental design was randomised with three to four replicates per treatment (Figure 1). Irrigation scheduling decisions for RDI were made independently on the basis of averaged Ψ_{rem} of each irrigation sector. Baselines for the calculation of CWSI and Ψ_{rem} were calculated in this study according to the equations provided by Bellvert et al. (2014b) in Chardonnay. Once the threshold was surpassed, the irrigation requirements were calculated according to the ratio between actual and threshold potential, as follows:

$$T_{rate} = 1 - \left(\frac{\psi_{rem}}{\psi_{thr}} \right) \quad (1)$$

where T_{rate} is the threshold rate, Ψ_{rem} is the remotely sensed estimated leaf water potential of the irrigation sector, and Ψ_{thr} is the established leaf water potential threshold for each treatment and phenological stage. Based on previous experience in managing irrigation in a vineyard adjacent to that in this study (Girona et al. 2006), different doses of water have been defined taking into account the response of the winegrape.

The idea is that actual plant water status should reach values similar to those defined by leaf water potential threshold between 1 and 2 weeks. Irrigation recommendations (IR) are defined in Table 1.

Crop evapotranspiration was calculated as the product of ETo Penman-Monteith (Allen et al. 1998) and crop coefficients (Kc). The Kc values were derived from previous experiments (Girona et al. 2006, Marsal et al. 2008). The applied coefficients were as follows: $Kc_1 = 0.2$ (from budburst on 15 April); $Kc_2 = 0.7$ (mid-season, from veraison on 20 July until harvest); and $Kc_3 = 0.3$ (at leaf fall at the end of October).

Airborne campaign

The airborne campaign was conducted with a thermal camera (FLIR SC655, FLIR Systems, Wilsonville, OR, USA) installed on an aircraft (CESSNA C172S EC-JYN). The software to acquire thermal images was developed at the Laboratory for Research Methods in Quantitative Remote Sensing (Quantalab, IAS-CSIC, Córdoba, Spain), as described in Zarco-Tejada et al. (2012). The camera had a resolution of 640×480 pixels, equipped with a 13.1-mm optics focal length yielding an angular field of view of 45° that delivered approximate ground resolution of 0.25 m. Spectral response was in the range of 7.5–13 µm. Weekly flights were conducted at 12:00 solar time (14:00 local time) from May to September at 150 m above ground level and a speed of 130 km/h. Fourteen flights were made over the course of the season. The flying pattern consisted of eight longitudinal lines of 1500 m separated by 60 m. Airborne data were calibrated geometrically as explained in Berni et al. (2009a). Temperature from pure vegetation pixels was extracted from the imagery using an automated object-based image analysis method. A threshold method based on temperature variability was used to generate regions of interest over each pure vine, selecting only vegetation pixels. An algorithm was applied afterwards to restrict the shapes of the objects, excluding crown edges and avoiding soil/vegetation mixed pixels. Crown temperature was used to calculate the CWSI, according to the methodology developed by Idso et al. (1981). The non-water stress baselines required to compute the CWSI were developed in this vineyard in a previous study (Bellvert et al. 2014b). Values of Ψ_{rem} were calculated afterwards from CWSI data following the methodology described by Bellvert et al. (2014a,b) and are summarised in Table 2. Spatial maps for both CWSI and Ψ_{rem} were interpolated by kriging. Information of the averaged Ψ_{rem} of each irrigation sector was available for irrigation decisions between 36 and 48 h after the acquisition of thermal images. Local atmospheric conditions [air temperature (T_a), relative humidity, barometric pressure, radiation, wind speed and rainfall] at the time of flights were measured with two portable weather stations (Watchdog 2000, Model 2475 Plant Growth Station, Spectrum Technologies, Plainfield, IL, USA) located on one side of the vineyard (Table 3). Vapour pressure deficit was calculated using the equation from Murray (1967).

Table 1. Irrigation recommendations for Chardonnay winegrapes according the threshold rate values defined in Equation 1.

T_{rate}	IR
$T_{rate} > 0.12$	60% ETc
$0.12 \geq T_{rate} > -0.12$	100% ETc
$-0.12 \geq T_{rate} > -0.30$	120% ETc
$T_{rate} \leq -0.30$	160% ETc

IR, irrigation recommendations; T_{rate}, threshold rate.

Field measurements

Concomitant to each flight, Ψ_L was measured in each irrigation sector with the aim of comparing Ψ_{rem} with a ground-based stress indicator. The Ψ_L of four vines was measured within each irrigation sector (Figure 1). Two fully expanded, bagged leaves exposed to direct sunlight were taken from each vine. Measure-

Table 2. Phenological equations of lower and upper limits for calculation of crop water stress index (Idso et al. 1981), and remotely sensed estimates of leaf water potential in Chardonnay winegrapes.

	Stage I	Stage II	Stage III	Postharvest
Lower limit	$T_c–T_a = -2.23VPD+3.64$	$T_c–T_a = -1.39VPD + 2.16$		$T_c–T_a = -1.29VPD + 1.55$
Upper limit	$T_c–T_a = 0.63VPD+6.61$	$T_c–T_a = 0.64VPD + 6.45$		$T_c–T_a = 0.21VPD+4.42$
Ψ_{rem} (MPa)	$-0.02CWSI^2 - 0.85CWSI - 0.50$	$-0.06CWSI^2 - 1.11CWSI - 0.56$	$-0.56CWSI^2 - 0.44CWSI - 0.71$	$-0.26CWSI^2 - 0.55CWSI - 0.79$

This information is provided from a previous study in the same vineyard (Bellvert et al. 2014b). CWSI, crop water stress index; $T_c–T_a$, corresponds to difference of canopy and air temperature; VPD, vapour pressure deficit; Ψ_{rem}, remotely sensed estimates of leaf water potential.

Table 3. Climate data at the 16-ha commercial Chardonnay vineyard during the flight times.

Date	DOY	Phenological stage	VPD (kPa)	Radiation (W/m^2)	Wind speed (m/s)	Rainfall last 72 h (mm)
23 May	143	I	1.6	932.0	2.1	9
30 May	150	I	2.9	921.1	1.7	0
6 Jun	157	I	2.3	953.7	1.3	0
13 Jun	164	I	2.3	987.8	2.5	0
20 Jun	171	II	1.6	932.7	1.0	15
29 Jun	180	II	3.3	935.6	1.6	0
4 Jul	185	II	2.8	943.9	1.6	0
11 Jul	192	II	2.3	933.0	1.1	0
18 Jul	199	II	4.1	971.3	1.2	0
25 Jul	206	II	2.8	934.0	1.4	0
31 Jul	212	III	2.1	872.5	1.1	0
7 Aug	219	III	2.5	845.0	0.9	18
16 Aug	228	PH	3.5	891.0	0.8	0
6 Sep	249	PH	3.0	753.9	1.4	0

DOY, day of the year; VPD, vapour pressure deficit.

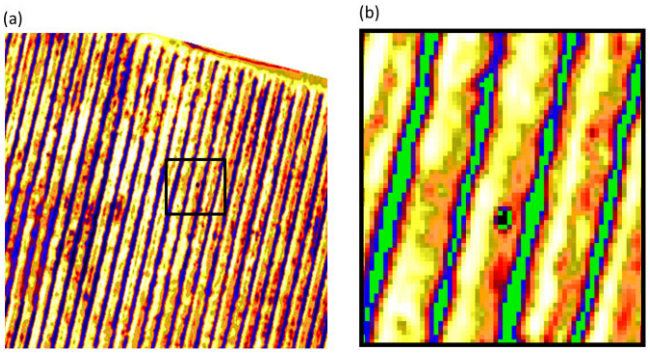

Figure 2. Thermal mosaic of a 16-ha commercial Chardonnay vineyard with 0.25-m pixel resolution, and showing (a) detailed image of measured winegrapes located with aluminium paper between rows; and (b) identification of pure-vine pixels extracted from the centre of the rows (—) and used to calculate the crop water stress index (CWSI). The acquired high-resolution imagery enabled extraction of the water stress indices with no shadow or background effects.

ments of Ψ_L were made with a Scholander pressure chamber (Model 3005, Soil Moisture Corp., Santa Barbara, CA, USA) following the recommendations of Williams and Araujo (2002). Two teams, each equipped with a pressure chamber on a truck, were employed to ensure all measurements could be taken in 1 h around the time of the flight. In each measured vine, aluminum paper was used between rows to mark the exact location where Ψ_L was measured (Figure 2). Canopy temperature (T_c) was extracted from pixel information of the same measured vines.

The volume of applied irrigation water was determined by reading the water meters (CZ2000-3M, Contazara, Zaragoza, Spain) in each irrigation sector on a weekly basis. One water meter was installed in a pipe from one row per each irrigation sector. A sample of 16 vines was hand-harvested on 9 August in each irrigation sector. Grapes were used to produce sparkling base wine, and alcohol strength at harvest was 10.5%. Bunches per vine were counted and total yield was weighed. Bunch fresh mass was estimated as vine yield divided by bunch number per vine. Samples of 100 berries per irrigation sector were taken to the laboratory and weighed. In contrast, complete sectors were mechanically harvested by Raimat winery on 2 different days. Sectors 1–5 were harvested on 11 August, and the remaining sectors on 19 August.

Composition of must and sparkling base wines

Microvinifications were conducted at the VITEC Wine Technology Park (Falset, Spain) on 40-kg samples of grapes from each irrigation sector. Grapes were pressed by a Willmes pneumatic press (Sigma model, Willmes, Lorsch, Germany). Pressure was applied until 50% of must yield was obtained. Must was fermented at 17°C and monitored with daily density control until total glucose and fructose concentration was lower than 0.5 g/L. Fermentation took approximately 12 days to complete. The musts and sparkling base wines were analysed at the same time for each sample. Alcohol strength, titratable acidity, turbidity, phenolic substances (Folin–Ciocalteu Index, expressed as mg/L epicatechin) and proteins were measured following the procedure of the Organisation Internationale de la Vigne et du Vin (Organisation Internationale de la Vigne et du Vin 1990). Foam quality of the sparkling base wines was measured by the Mosalux method (Maujean et al. 1990). The measured foam parameter corresponded to foam height at stability (Hs), representing foam persistence.

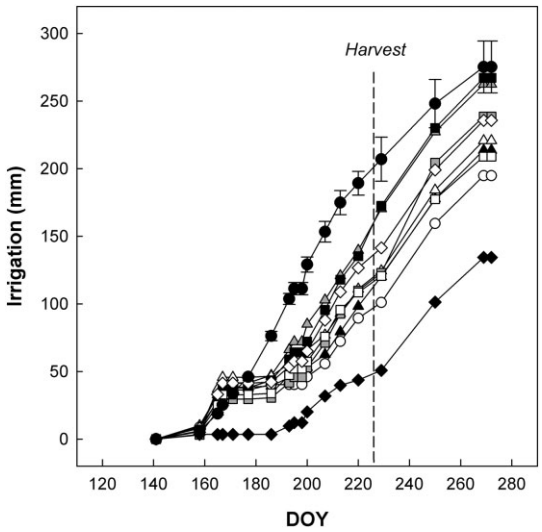

Figure 3. Seasonal patterns of cumulative applied water in each irrigation treatment of a 16-ha commercial Chardonnay vineyard: control (●); regulated deficit irrigation with a weekly scheduling (RDI-W) sector 3 (■), sector 7 (□), sector 9 (▩) and sector 12 (◇); regulated deficit irrigation with a biweekly scheduling (RDI-BW) sector 2 (▲), sector 4 (Δ), sector 6 (▲) and sector 10 (○); and in the sector under a severe deficit irrigation strategy (DI-W) (◆).

Results

Applied water

The averaged amount of applied water was 277, 235 and 221 mm for control, RDI-W and RDI-BW, respectively. The water saving of RDI treatments in comparison with control was between 15 and 20% (Figure 3). Water applied for the DI-W treatment was 134 mm, 51% less than that for the control.

Seasonal variation of measured and estimated leaf water potential

The pattern of measured (Ψ_L) and remotely estimated (Ψ_{rem}) leaf water potential remained consistent throughout the season for the different irrigation treatments (Figure 4). This relationship will be presented and analysed properly later. The main differences were found for the first four flights, corresponding to stage I. The control treatment presented the greatest difference between Ψ_L and Ψ_{rem}, with a root mean square error (RMSE) of 0.22 MPa over the growing season (Figure 4a). Leaf water potential decreased during stage II for the RDI treatments from the flight on day of the year (DOY) 180 (Figure 4b,c). During stage II, RMSE for the RDI treatments was 0.17 MPa. During stage III, differences in the estimate of Ψ_L were most notable on DOY 212 and 219 for the three treatments. For the data from those two days, RMSE was 0.30 MPa. During the postharvest period, a slight difference was detected between Ψ_L and Ψ_{rem} on DOY 249. The sector under DI-W had a consistent seasonal pattern in Ψ_{rem} and RMSE was 0.11 MPa (Figure 4d).

Irrigation scheduling based on remotely sensed Ψ_L

Measured leaf water potential (Ψ_L) revealed a clear difference between irrigation treatments (Figure 4). During the early part of the season, there was no significant difference between treatments, and all Ψ_L values were above −0.7 MPa. Fully irrigated sectors (control) had an Ψ_L value above −0.7 MPa throughout the season, except immediately after harvest when Ψ_L fell to −0.9 MPa. Regulated deficit irrigation treatments (RDI-W and RDI-BW) affected midday Ψ_L during stage II, which decreased to a minimum value of −1.0 MPa on DOY 180 and remained fairly constant until re-watering during stage III and postharvest,

reaching a final value of −0.8 MPa. Seasonal evolution of Ψ_L values of both RDI treatments did not differ significantly ($P = 0.643$). For the sector under severe deficit irrigation (DI-W), Ψ_L decreased progressively from the beginning of stage II until harvest, reaching a minimum value of −1.2 MPa during the last 3 weeks before harvest. Similarly to the other treatments, Ψ_L fell to −1.4 MPa immediately after harvest, and recovered for the last measurement.

The maps of Ψ_{rem} illustrate the spatial variability of vine water status within the vineyard, according to the different irrigation treatments (Figures 5,6). During stage I, the averaged

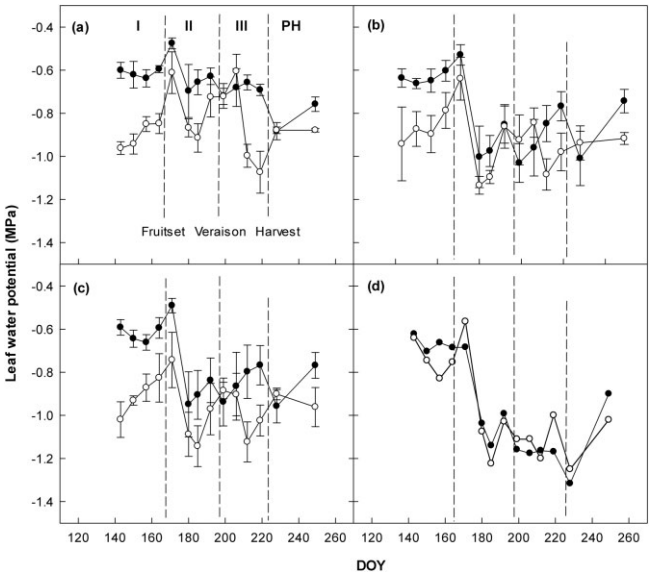

Figure 4. Seasonal variation of measured (Ψ_L) (●) and remotely sensed estimated (Ψ_{rem}) (○) midday leaf water potential during phenological stages I, II, III and postharvest for (a) control, (b) regulated deficit irrigation with a weekly scheduling (RDI-W), (c) regulated deficit irrigation with a biweekly scheduling (RDI-BW) and (d) severe deficit irrigation treatments of a 16-ha commercial Chardonnay vineyard. Values reported are treatment means ± standard error of eight determinations.

Ψ_{rem} value for each irrigation sector did not show any significant difference between irrigation treatments (Figures 5a,6a); Ψ_{rem} values ranged between −0.66 and −0.84 MPa, and were similar to established Ψ_{thr} for stage I. The corresponding maps during stage II showed a clear difference in the spatial variability of vine water status between irrigation treatments (Figures 5b,c,6b,c). At the beginning of stage II, control sectors (1, 5 and 8) displayed higher Ψ_{rem} values in comparison with those under RDI on a weekly (Figure 5b) and biweekly basis (Figure 6b). Averaged Ψ_{rem} values for most sectors under RDI were similar to established Ψ_{thr}, with the exception of sectors 3, 4 and 9, which had slightly lower Ψ_{rem} values than Ψ_{thr}.

Maximum stress throughout the season was detected on the flight of 4 July (Figures 5c,6c). Most of the irrigation sectors under RDI had a Ψ_{rem} below the Ψ_{thr} defined at that moment. As a result, irrigation water supply consisted of over-irrigating sectors 2, 3, 9, 10 and 12 to 120% ETc, and sector 4 to 160% ETc (Figures 5g,6g). The irrigation sector under DI-W reached the minimum value ($\Psi_{rem} = -1.24$ MPa) that corresponded to the established Ψ_{thr} for this treatment. Hence, this irrigation sector was also fully irrigated until harvest in order to maintain similar Ψ_{rem} values (Figure 5g). On 16 August, some sectors within the vineyard were completely harvested (1–5). The phenological differences affected leaf temperature (T_c) by increasing averaged T_c–T_a values in the harvested sectors (data not shown). As a result, the algorithms for the calculation of CWSI and Ψ_{rem} were applied according to the phenology of each irrigation sector. At that moment (DOY 228), T_{rate} for all sectors ranged between −0.12 and −0.30, and applied irrigation water was around 120% ETc until the next flight (Figures 5h,6h).

Yield and base wine composition

No significant difference was found between irrigation treatments in yield parameters (data not shown). Yield ranged from 7.1 to 8.5 kg/vine, and the number of bunches per vine and berry fresh mass at harvest was approximately 38 bunches/vine and 1.6 g/vine, respectively. Although not statistically significant, it appears that the yield of the DI-W treatment was slightly

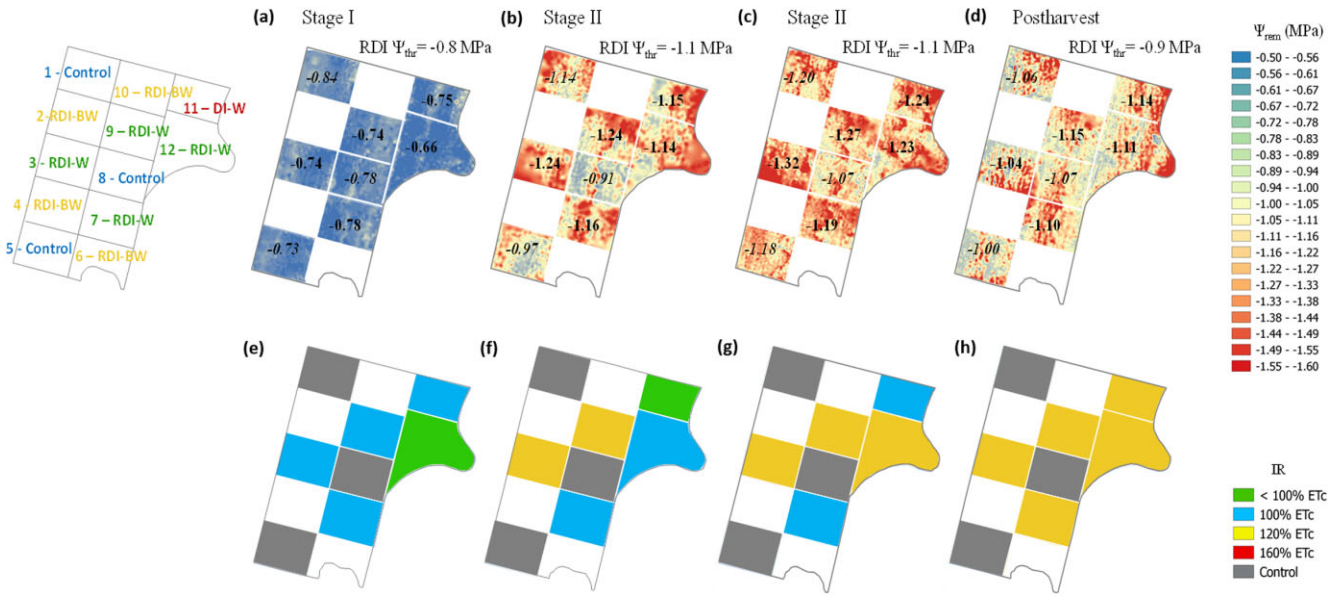

Figure 5. Spatial variability of vine water status, obtained from high-resolution airborne thermal images, of a 16-ha commercial Chardonnay vineyard at (a, e) stage I [day of the year (DOY) 164], (b, f) stage II (DOY180), (c, g) stage II (DOY185) and (d, h) postharvest (DOY228) phenological stages, with (a–d) showing remotely sensed estimated leaf water potential (Ψ_{rem}) of Control and regulated deficit irrigation with a weekly scheduling (RDI-W) treatments, as well as of the sector under a severe deficit irrigation (DI-W), and with (e–h) illustrating the proposed irrigation requirements (IR) for each of the irrigation sectors. Values within each irrigation sector correspond to estimated leaf water potential (Ψ_{rem}), with irrigation sectors (■) corresponding to the control treatment. Leaf water potential thresholds (Ψ_{thr}) correspond to RDI treatments.

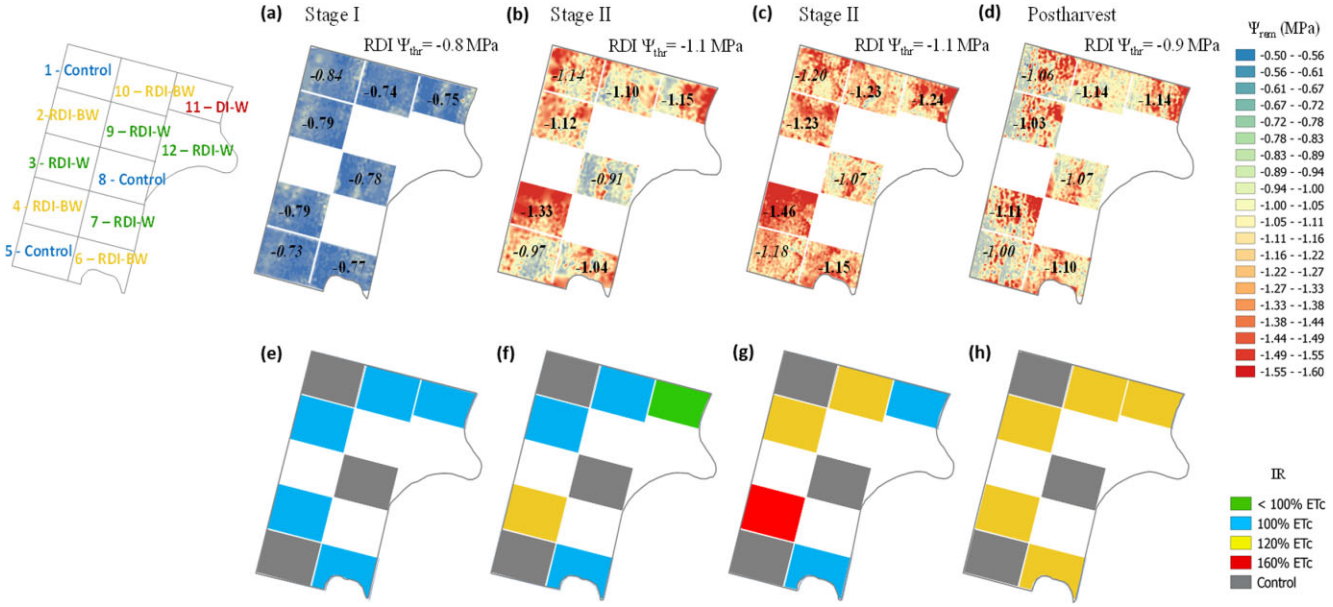

Figure 6. Spatial variability of vine water status, obtained from high-resolution airborne thermal images, of a 16-ha commercial Chardonnay vineyard at (a, e) stage I [day of the year (DOY) 164], (b, f) stage II (DOY180), (c, g) stage II (DOY185) and (d, h) postharvest (DOY228) phenological stages showing remotely sensed estimated leaf water potential (Ψ_{rem}) of control and regulated deficit irrigation with a biweekly scheduling (RDI-BW) treatments, as well as of the sector under a severe deficit irrigation (DI-W), and with (e–h) illustrating proposed irrigation requirements (IR) for each of the irrigation sectors. Values within each irrigation sector correspond to estimated leaf water potential values (Ψ_{rem}) and with irrigation sectors (■) corresponding to the control treatment. Leaf water potential thresholds (Ψ_{thr}) correspond to RDI treatments.

lower than that of the others. The composition of both must and sparkling base wine showed no significant difference between the irrigation treatments. The sampled 16 vines of each treatment were harvested on the same day, and although the differences were not significant the berries of vines under DI-W had a slightly higher alcohol and phenolic substances concentration, but less titratable acidity and turbidity.

Discussion

Irrigation scheduling based on remotely sensed Ψ_L

In semi-arid winegrowing regions, an optimum irrigation management strategy requires information on the vine water status and the ability to assess the adequacy of irrigation intensity during the growing season (Grimes and Williams 1990). Combining information from the water balance method (Allen et al. 1998) with leaf water potential adjustments for triggering irrigation (Girona et al. 2006) may be a feasible technique for the adoption of precision irrigation strategies.

This study demonstrated that irrigation scheduling of RDI treatments, based on supplying a different proportion of ETc when Ψ_{rem} values were more negative than the established Ψ_{thr}, provided substantial advantages to account for spatial variability. Figure 4 shows how Ψ_{rem} had a similar trend to measured Ψ_L for all treatments from fruitset (stage II), except for those days with low VPD or after rainfall (DOY 212 and 219) (Table 3). The effect of VPD on estimation of Ψ_{rem} for these 2 days is explained below. In addition, no difference was detected in terms of measured leaf water potential for those RDI treatments scheduled on a weekly or biweekly basis (Figure 7). These results suggest that the acquisition of thermal images on a weekly basis is not justified in this vineyard. In terms of cost efficiency, the elaboration of five to six thermal flights during the season would be the best solution as a decision support to schedule irrigation. The cost of this technology is discussed further. The starting date, however, for acquiring thermal images may be relevant since error estimations were large until DOY 170. This effect

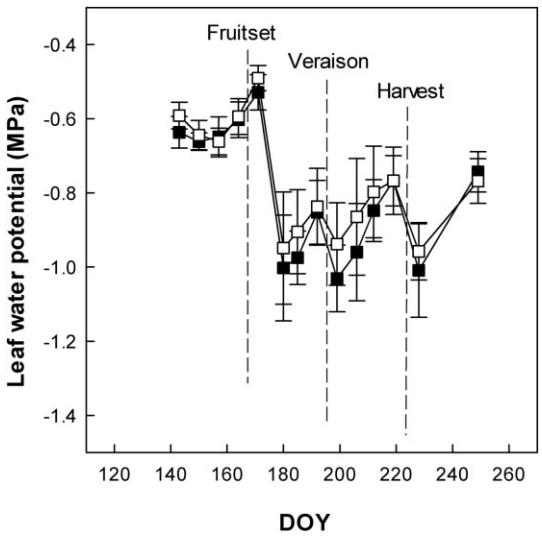

Figure 7. Seasonal variation of measured leaf water potential for irrigation treatments under regulated deficit irrigation (RDI), scheduled on a weekly (RDI-W) (■) and biweekly (RDI-BW) (□) basis. Values reported are treatment means ± standard error of eight determinations. DOY, day of the year.

may be due to the difficulty of extracting pure vegetation pixels when the canopy is not fully developed (Figure 8). In some zones within the vineyard, the width of the vegetation canopy during stage I was about 0.35 m. Because pixel size was 0.25 m, the number of pure vegetation canopy pixels selected in the early stages was possibly lower than in subsequent stages, and mixed information coming from leaves, soil and shadow background would probably affect the CWSI calculation. Bellvert et al. (2014a) demonstrated that, for a range of 0.3–2.0 m, 0.30-m pixel size performed best in terms of differentiating canopy temperature from soil temperature in vineyards. Therefore, until further improvement in spatial resolution is feasible (i.e. pixel size smaller than 0.25 m), the starting date for this

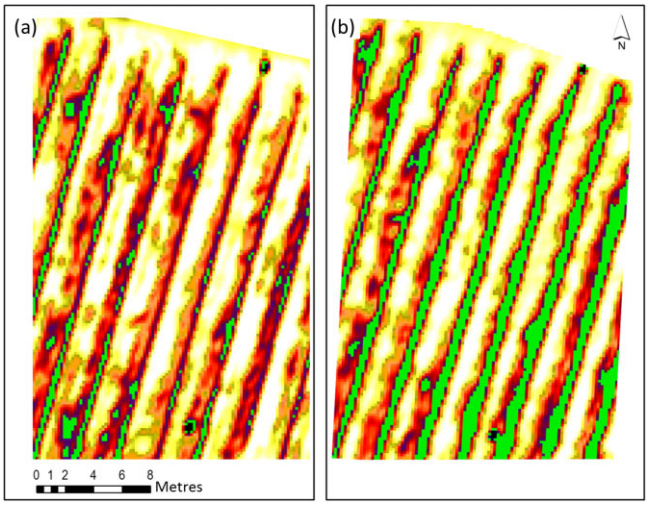

Figure 8. Detail of the pure-vine vegetation pixels used for calculating the crop water stress index (CWSI) at two different moments of the season, (a) day of the year (DOY) 150 (stage I) and (b) DOY 206 (stage III).

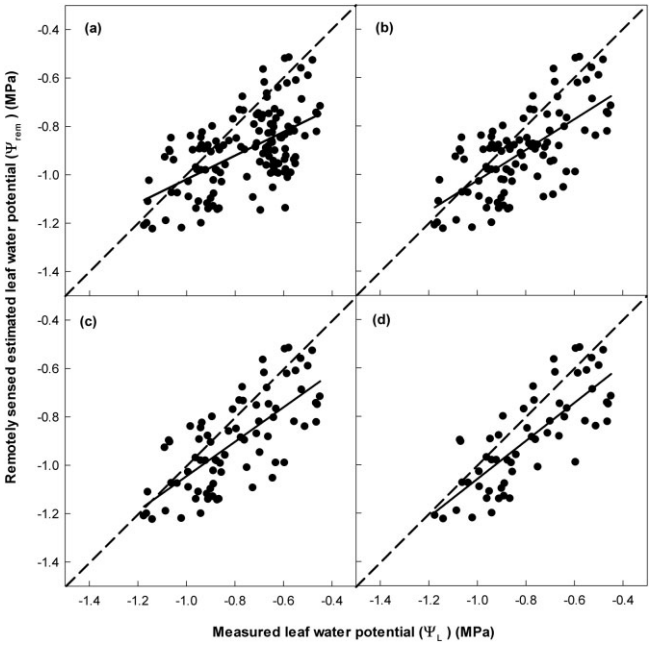

Figure 9. Relationships between measured (Ψ_L) and remotely sensed estimated (Ψ_{rem}) leaf water potential in a 16-ha commercial Chardonnay vineyard, showing (a) data from all the seasons ($R^2 = 0.31$, y = 0.49x – 0.53, $P < 0.0001$, RMSE = 0.21); (b) data from stages II, III and postharvest ($R^2 = 0.44$, y = 0.63x – 0.39, $P < 0.0001$, RMSE = 0.17); (c) data from stages II and III ($R^2 = 0.51$, y = 0.71x – 0.33, $P < 0.0001$, RMSE = 0.17), and (d) data from stages II and III, with the exception of data from DOY 219 and other days with vapour pressure deficit below 2.3 kPa ($R^2 = 0.61$, y = 0.78x – 0.27, $P < 0.0001$, RMSE = 0.15). DOY, day of the year; RMSE, root mean square error.

methodology must be adapted according to canopy size (around the beginning of stage II, for the conditions of this experiment).

The seasonal validation of the estimated versus field-measured Ψ_L values are shown in Figure 9. Validation using all data resulted in an underestimation of Ψ_L compared with field measurements (Figure 9a). A slight improvement took place when data from stage I were removed (Figure 9b). The relationship was further improved when the data of stages II–III corresponding to low VPD or days after rainfall were excluded from the analysis (Figure 9d). Hence, these results suggest that the optimal seasonal moment for remote detection of vine water status is during stages II–III. During

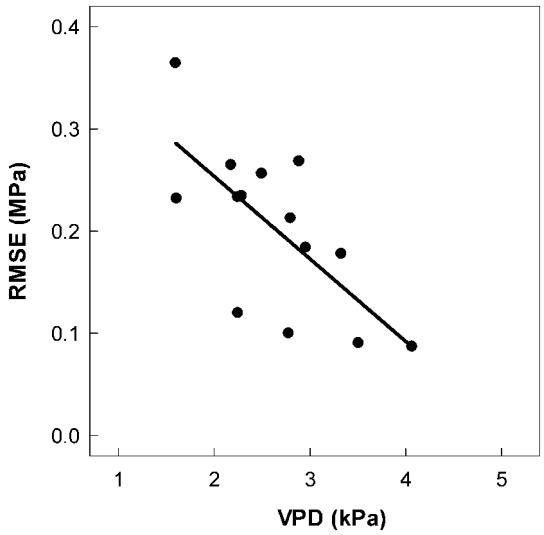

Figure 10. Effect of vapour pressure deficit (VPD) on remotely sensed estimates of leaf water potential (Ψ_{rem}) in a 16-ha commercial Chardonnay vineyard. RMSE corresponded with the root mean square error between measured and remotely estimated leaf water potential ($R^2 = 0.49$, y = 0.081x – 0.415, $P < 0.005$).

Table 4. Relationship between root mean square error and vapour pressure deficit during stages II–III of the Chardonnay winegrapes.

VPD range	VPD (kPa)	RMSE
<2.0	1.61	0.23
2.0–2.2	2.22	0.19
2.2–2.5	2.25	0.12
2.5–3.0	2.79	0.16
>3.0	3.70	0.13

RMSE, root mean square error; VPD, vapour pressure deficit.

postharvest, the relationship between estimated and measured Ψ_L may be affected both by defoliation caused by the mechanical winegrape harvester and transpiration reduction due to sink removal at harvest, which lowers vine water consumption (Reyes et al. 2006, Marsal et al. 2008). In fact, this postharvest effect was evident in the thermal mosaic acquired on 16 August (DOY 228) due to the fact that only a few sectors within the vineyard were harvested (1–5) (Figures 5d,6d).

Effect of VPD on Ψ_{rem}

Some authors have mentioned that one of the limitations of CWSI is that its precision is climate-dependent (Hipps et al. 1985), suggesting that the use of this index is not recommended in humid climates and in environments with significant climatic variability (Jones 2004, Testi et al. 2008). The results of this study show that low VPD had a negative effect on the remote estimation of Ψ_L. The RMSE between measured and estimated Ψ_L for all seasonal data was lower as VPD increased (Figure 10). Most of the low VPD values occurred during early season, when the use of thermal imagery was limited by the spatial resolution of the camera. Even when the canopy was fully developed, however, low VPD values affected the estimation of Ψ_{rem} (Figure 9c,d). Those days of stages II–III with a VPD value below 2 kPa presented an averaged RMSE of 0.23 MPa, while RMSE decreased as the VPD range increased (Table 4). The lowest VPD values during stages II–III were 2.1, 2.3 and 2.5 kPa corresponding to days 212, 192 and 219, respectively (Table 3). Radiation for two of these days was also lower in comparison with previous flights, and a rainfall of 18 mm occurred 2 days before DOY 219. The rainfall

may have modified the VPD and air temperature within the vineyard at the flight time as water evaporated from soil and vegetation surfaces. Consequently, the evaporative demand within the vineyard may be lower than in the location where the weather station was installed. If that would be the case, the data from the weather station would produce estimates of CWSI indicative of more negative Ψ_{rem} values. Differences between estimated and measured Ψ_L, however, for these days with low VPD were apparent in all treatments except for DI-W (Figure 4). Our hypothesis is that the signal (T_c–T_a) is higher in stressed than in well-watered winegrapes. This is equally true for VPD, and explains why leaf water potential can be more precisely estimated by thermal imagery in stressed winegrapes. Finally, we consider that the slight difference between Ψ_L and Ψ_{rem} in the last flight of day 249 was probably caused by a soil background effect due to broken leaves after mechanical harvest.

Water applied, yield and wine composition

Variability of irrigation water applied throughout the season was high between all irrigation sectors within the vineyard (coefficient of variability, CV = 19%), ranging from 135 to 300 mm. Comparing the variability of the amount of water applied in irrigation treatments under the water balance method (control) with the other treatments, those irrigated using Ψ_L as the irrigation trigger (RDI) had a CV of around 18%, while the CV for control was 6%. Despite that, the same amount of water was scheduled in the three control sectors; water meter readings were measured only in one row per irrigation sector. Spatial variability between rows (i.e. topography) could explain the variability in water applied between the control sectors. These results mean that by adopting the same irrigation strategy based on maintaining specific Ψ_L thresholds, different amounts of water would be needed in the different irrigation sectors. The main advantage of using plant water status indicators such as Ψ_L over the water balance method is that it provides site-specific information of vine water status and takes into account spatial variability of the vineyard. These results show that scheduling irrigation by using remotely sensed Ψ_L thresholds can increase the precision of irrigation within a vineyard. Despite the adoption of mild deficit irrigation strategies during a single year, which implied important water savings, no significant difference was detected in either yield or wine composition parameters. It is likely that an impact on yield would be seen in a longer term application of RDI. In addition, it may be that 16 harvested winegrapes were insufficient and/or not representative of the whole irrigation sector because of the large spatial variability within sectors. In fact, when comparing the within sector averaged spatial variability in the vineyard on the day of the season with a maximum stress (DOY 185) with averaged spatial variability between sectors of control and RDI-W, the coefficient of variation (CV) was, respectively, 9.1% reduced up to 5.1%. This demonstrated that spatial variability within a plot was greater than between plots, when irrigation was scheduled on a weekly basis. Taking into account that vineyard heterogeneity is higher when an RDI strategy rather than a full irrigation is applied (Bellvert et al. 2012), this study demonstrates the importance of managing differentially irrigation sectors on a weekly basis when RDI is adopted. However, CV between sectors under RDI-BW reached 10.2%, mostly because of irrigation sector number 4, which reached Ψ_L values more negative than Ψ_{thr}. This reveals one of the limitations of scheduling irrigation on a biweekly basis, when RDI is applied in shallower soils.

Finally, it was worth pointing out the cost-effectiveness of this technology in the viticulture sector. The cost to apply this tool in the 16-ha vineyard studied is detailed in Table 5. Probably, for many years the weaknesses of using thermal remote sensing in viticulture has been the scarcity of cameras with high spatial resolution, the prohibitive cost of flying with aircraft (this may vary between countries), and finally the little time available for the interpretation and delivering support decisions to the viticulturists. In this study, Ψ_L maps and IRs for each individual sector were delivered between 36 and 48 h after the flight. The estimated final cost per hectare and flight was €25. Since this study demonstrated that the best solution to complete a growing season was between five to six flights, the annual final cost can be around €125–150/ha. It is true, however, that costs may depend on area to be covered. For instance, we expect a lower cost for large areas and nearby vineyards. Also note that this is the current cost of using a thermal camera of 640 × 480 pixel resolution, which needs the aircraft to fly at 150 m above ground level to deliver pixels of 0.25 m. In the coming years, it is expected that the necessary time for flying and per-hectare cost will likely be reduced, since new thermal cameras with a higher resolution are already on the verge of being available. It should be emphasised that this tool enables the reduction of vineyard spatial heterogeneity by adopting a differential irrigation management as well as the adoption of optimal irrigation strategies for each specific cultivar throughout the season. The improvement on berry composition and water savings justifies the cost and maximises the benefits to the wine industry.

Table 5. Detailed description of the estimated costs per hectare and flight, for the 16-ha Chardonnay vineyard.

N°	Tasks	Time (h)	Cost (€/h)	Cost (€)/ vineyard
1	Flight planning	0.5	22†	11
2	Installation of sensors and flight set-up	1	22	22
3	Flight and image acquisition	0.5	350	175
4	Download weather station data and upload images to server	1	22	22
5	Image processing	7	22	154
6	Upload to server and customer delivery	0.5	22	11
	Total	10.5		395
	Total cost (€/ha)		25	

†It has been assumed that the cost of a technician is 22 €/h.

Conclusions

This study demonstrated that scheduling irrigation of a vineyard throughout a season according to remotely sensed leaf water potential quantified from a thermal cost-effective camera is feasible. This method enabled the development of RDI strategies in Chardonnay vines without any negative effect on yield and wine composition. Moreover, this study verified that a similar vine water status was maintained when management decisions were taken on a biweekly basis. Some constraints, however, should be considered for the implementation of this technology in viticulture. These are the following: (i) high spatial resolution thermal imagery is required for scheduling irrigation of a vineyard during a complete growing season, especially during the early stages; (ii) acquisition of thermal images on days after rainfall may be a source of error for remotely detecting vine water status; and (iii) days with low VPD values (<2.3 kPa) negatively influenced the remote estimation of leaf water potential derived from CWSI.

Acknowledgements

This research was supported by the Spanish Ministry of Economy and Competitiveness, under Project INNPACTO IPT-2011-1786-060000. We are grateful for the collaboration of Codorniu winery and Sorigué, S.A. in carrying out this study. The work of the company RS Aviation, and in particular of Mr Robert Pedra, is gratefully acknowledged. In addition to these companies, the authors would like to thank the staff of Quantalab at IAS-CSIC for their technical support in processing the thermal images, and Mrs Mercè Mata, Mr Carles Paris, Miss Núria Bonastre, Miss Núria Civit, Mr Gerard Piñol and Mr Jordi Oliver, who are members of the staff of the Efficient Use of Water program at IRTA for measurements and technical support in the field campaign.

References

Acevedo-Opazo, C., Tysseyre, B., Taylor, J., Ojeda, H. and Guillaume, S. (2010) Spatial prediction model of the vine (*Vitis vinifera L.*) water status using high resolution ancillary information. Precision Agriculture **11**, 358–378.

Allen, R.G., Pereira, L.S., Raes, D. and Smith, M. (1998) Crop evapotranspiration. Guidelines for computing crop water requirements. FAO Irrigation and Drainage Paper No. 56, Food and Agriculture Organization, Rome, Italy.

Basile, B., Marsal, J., Mata, M., Vallverdú, X., Bellvert, J. and Girona, J. (2011) Phenological sensitivity of Cabernet Sauvignon to water stress: vine physiology and berry composition. American Journal of Enology and Viticulture **62**, 452–461.

Basile, B., Girona, J., Behboudian, M.H., Mata, M., Roselló, J., Ferré, M. and Marsal, J. (2012) Responses of 'Chardonnay' to deficit irrigation applied at different phenological stages: vine growth, must composition, and wine quality. Irrigation Science **30**, 397–406.

Bellvert, J., Marsal, J., Mata, M. and Girona, J. (2012) Identifying irrigation zones across a 7.5-ha 'Pinot noir' vineyard based on the variability of vine water status and multispectral images. Irrigation Science **30**, 499–509.

Bellvert, J., Zarco-Tejada, P.J., Girona, J. and Fereres, E. (2014a) Mapping crop water stress index in a 'Pinot-noir' vineyard: comparing ground measurements with thermal remote sensing imagery from an unmanned aerial vehicle. Precision Agriculture Journal **15**, 361–376.

Bellvert, J., Zarco-Tejada, P.J., Girona, J., Marsal, J. and Fereres, E. (2014b) Seasonal evolution of crop water stress index in grapevine varieties determined with high resolution remote sensing thermal imagery. Irrigation Science **33**, 81–93.

Berni, J.A., Zarco-Tejada, P.J., Suarez, L. and Fereres, E. (2009a) Thermal and narrow-band multispectral remote sensing for vegetation monitoring from an unmanned aerial vehicle. IEEE Transactions on Geoscience and Remote Sensing **47**, 722–738.

Berni, J.J., Zarco-Tejada, P.J., Sepulcre-Cantó, G., Fereres, E. and Villalobos, F. (2009b) Mapping canopy conductance and CWSI in olive orchards using high resolution thermal remote sensing imagery. Remote Sensing of Environment **113**, 2380–2388.

Bramley, R.G.V. and Hamilton, R.P. (2004) Understanding variability in winegrape production systems. 1. Within vineyard variation in yield over several vintages. Australian Journal of Grape and Wine Research **10**, 32–45.

Bramley, R.G.V., Proffitt, A.P.B., Hinze, C.J., Pearse, B. and Hamilton, R.P. (2005) Generating benefits from precision viticulture through selective harvesting. Stafford, J.V., ed. Precision agriculture '05. Proceedings of the 5th European conference on precision agriculture; 9–12 June; Uppsala, Sweden (Wageningen Academic Publishers: Wageningen, The Netherlands) pp. 891–898.

Fuchs, M. and Tanner, C.B. (1966) Infrared thermometry of vegetation. Agronomy Journal **58**, 297–601.

Ginestar, C., Eastham, J., Gray, S. and Iland, P.G. (1998) Use of sap-flow sensors to schedule vineyard irrigation. II. Effects of post-veraison water deficits on composition of Shiraz grapes. American Journal of Enology and Viticulture **49**, 421–428.

Girona, J., Marsal, J., Mata, M., del Campo, J. and Basile, B. (2009) Phenological sensitivity of berry growth and composition of Tempranillo grapevines (*Vitis vinifera* L.) to water stress. Australian Journal of Grape and Wine Research **15**, 268–277.

Girona, J., Mata, M., del Campo, J., Arbonés, A., Bartra, E. and Marsal, J. (2006) The use of midday leaf water potential for scheduling deficit irrigation in vineyards. Irrigation Science **24**, 115–127.

Grimes, D.W. and Williams, L.E. (1990) Irrigation effects on plant water relations and productivity of 'Thompson Seedless' grapevines. Crop Science **30**, 255–260.

Hipps, L.E., Asrar, G. and Kanemasu, E.T. (1985) A theoretically-based normalization of environmental effects on foliage temperature. Agricultural and Forest Meteorology **27**, 59–70.

Idso, S.B., Jackson, R.D., Pinter, P.J., Reginato, R.J. and Hatfield, J.L. (1981) Normalizing the stress-degree day parameter for environmental variability. Agricultural Meteorology **24**, 45–55.

Intrigliolo, D. and Castel, J.R. (2010) Response of grapevine cv. 'Tempranillo' to timing and amount of irrigation: water relations, vine growth, yield and berry and wine composition. Irrigation Science **28**, 113–125.

Jackson, R.D., Idso, S., Reginato, R. and Pinter, P. Jr. (1981) Canopy temperature as a crop water stress index indicator. Water Resources Research **17**, 1133–1138.

Jones, H.G. (2004) Irrigation scheduling: advantages and pitfalls of plant-based methods. Journal of Experimental Botany **55**, 2427–2436.

Marsal, M., Mata, M., del Campo, J., Arbones, A., Vallverdú, X., Girona, J. and Olivo, N. (2008) Evaluation of partial root-zone drying for potential field use as a deficit irrigation technique in commercial vineyards according to two different pipeline layouts. Irrigation Science **26**, 347–356.

Maujean, A., Poinsaut, P., Dantan, H., Brissonnet, F. and Cossiez, E. (1990) Etude de la tenue et de la qualité de mousse des vins effervescents. II. Mise au point d'une technique de mesure de la moussabilité, de la tenue et de la stabilité de la mousse des vins effervescents. Bulletin de l'OIV **63**, 405–426.

Möller, M., Alchanatis, V., Cohen, Y., Meron, M., Tsipris, J., Naor, A., Ostrovsky, V., Sprintsin, M. and Cohen, S. (2007) Use of thermal and visible imagery for estimating crop water status of irrigated grapevine. Journal of Experimental Botany **58**, 827–838.

Murray, F.W. (1967) On the computation of saturation vapor pressure. Journal of Applied Meteorology **6**, 203–204.

Ojeda, H., Carrillo, N., Deis, L., Tisseyre, B., Heywang, M. and Carbonneau, A. (2005) Viticulture de precision et at hydrique. II: comportement quantitative et qualitative de zones intra-parcellaires définies à partir de la cartographie des potentiels hydriques. XIV International GESCO viticulture congress; 23-27 August 2005; Geisenheim, Germany (Groupe Europeen d'Étude des Systèmes de Conduite de la Vigne: Geisenheim, Germany) pp. 741–748.

Organisation Internationale de la Vigne et du Vin (1990) Recueil des méthods internationales d'analyse des vins et des môuts (Organisation Internationale de la Vigne et du Vin: Paris, France).

Reyes, V., Girona, J. and Marsal, J. (2006) Effect of late Spring defruiting on net CO_2 exchange and leaf area development in apple tree canopies. Journal of Horticultural Science & Biotechnology **81**, 575–582.

Sepulcre-Cantó, G., Zarco-Tejada, P.J., Jimenez-Muñoz, J., Sobrino, J., de Miguel, E. and Villalobos, F.J. (2006) Detection of water stress in a olive orchard with thermal remote sensing imagery. Agricultural and Forest Meteorology **136**, 31–44.

Sepulcre-Cantó, G., Zarco-Tejada, P.J., Jiménez-Muñoz, J.C., Sobrino, J.A., Soriano, M.A., Fereres, E., Vega, V. and Pastor, M. (2007) Monitoring yield and fruit quality parameters in open-canopy tree crops under water stress. Implications for ASTER. Remote Sensing of Environment **107**, 455–470.

Tanner, C.B. (1963) Plant temperatures. Agronomy Journal **55**, 210–211.

Testi, L., Goldhamer, D.A., Iniesta, F. and Salinas, M. (2008) Crop water stress index is a sensitive water stress indicator in pistachio trees. Irrigation Science **26**, 395–405.

US Department of Agriculture-Soil Conservation Service (1975) Soil taxonomy: a basic system of soil classification for making and interpreting soil surveys. United States Department of Agriculture Handbook, Vol. 436 (United States Government Printing Office: Washington, DC, USA).

Van Leeuwen, C., Tregoat, O., Choné, X., Bois, B., Pernet, D. and Gaudillère, J.P. (2009) Vine water status is a key factor in grape ripening and vintage quality for red bordeaux wine. How can it be assessed for vineyard management purposes? Journal International des Sciences de la Vigne et du Vin **43**, 121–134.

Williams, L.E. and Araujo, F.J. (2002) Correlations among predawn leaf, midday leaf, and midday stem water potential and their correlations with other measures of soil and plant water status in *Vitis vinifera*. Journal of the American Society for Horticultural Science **127**, 448–454.

Zarco-Tejada, P.J., González-Dugo, V. and Berni, J.A.J. (2012) Fluorescence, temperature and narrow-band indices acquired from a UAV platform for water stress detection using a micro-hyperspectral imager and a thermal camera. Remote Sensing of Environment **117**, 322–337.

Zarco-Tejada, P.J., Berni, J.A., Suárez, L., Sepulcre-Cantó, G., Morales, F. and Miller, J.R. (2009) Imaging chlorophyll fluorescence with an airborne narrow-band multispectral camera for vegetation stress detection. Remote Sensing of Vegetation **113**, 1262–1275.

Manuscript received: 5 August 2014

Revised manuscript received: 24 January 2015

Accepted: 21 May 2015